symmetry

MDPI

Article

Decoherence Effects in a Three-Level System under Gaussian Process

Sultan M. Zangi [1,†], Atta ur Rahman [2,*,†], Zhao-Xo Ji [3], Hazrat Ali [4] and Huan-Guo Zhang [3]

[1] School of Physics and Astronomy, Yunnan University, Kunming 650500, China
[2] School of Physics, University of Chinese Academy of Sciences, Yuquan Road 19A, Beijing 100049, China
[3] Key Laboratory of Aerospace Information Security and Trusted Computing, Ministry of Education, School of Cyber Science and Engineering, Wuhan University, Wuhan 430072, China
[4] Department of Physics, Abbottabad University of Science and Technology, Havellian P.O. Box 22500, Pakistan
* Correspondence: attapk@outlook.com
† These authors contributed equally to this work.

Abstract: When subjected to a classical fluctuating field characterized by a Gaussian process, we examine the purity and coherence protection in a three-level quantum system. This symmetry of the three-level system is examined when the local random field is investigated further in the noiseless and noisy regimes. In particular, we consider fractional Gaussian, Gaussian, Ornstein–Uhlenbeck, and power law noisy regimes. We show that the destructive nature of the Ornstein–Uhlenbeck noise toward the symmetry of the qutrit to preserve encoded purity and coherence remains large. Our findings suggest that properly adjusting the noisy parameters to specifically provided values can facilitate optimal extended purity and coherence survival. Non-vanishing terms appear in the final density matrix of the single qutrit system, indicating that it is in a strong coherence regime. Because of all of the Gaussian noises, monotonic decay with no revivals has been observed in the single qutrit system. In terms of coherence and information preservation, we find that the current qutrit system outperforms systems with multiple qubits or qutrits using purity and von Neumann entropy. A comparison of noisy and noiseless situations shows that the fluctuating nature of the local random fields is ultimately lost when influenced using the classical Gaussian noises.

Keywords: coherence; three-level system; classical fluctuating field; Gaussian process; purity

Citation: Zangi, S.M.; ur Rahman, A.; Ji, Z.-X.; Ali, H.; Zhang, H.-G. Decoherence Effects in a Three-Level System under Gaussian Process. *Symmetry* **2022**, *14*, 2480. https://doi.org/10.3390/sym14122480

Academic Editors: Wuming Liu and Xingdong Zhao

Received: 28 October 2022
Accepted: 15 November 2022
Published: 23 November 2022

1. Introduction

In recent decades, there has been considerable progress in quantum information processing and quantum computing [1–3], inspired by the design and enhancement of certain related aspects [4–6]. Quantum coherence has remained one of the most active research areas in quantum information sciences, and it has been extensively investigated, yielding significant results and improvements in quantum mechanical protocols [7,8]. Coherence preservation in a quantum system ensures successful transmission and higher efficiency in practical quantum information processing. The concept of super-positioning is central to quantum physics and quantum computing, and is referred to as quantum coherence. Coherence has also been found to be a requirement for entanglement and other types of quantum correlations [9–14].

The entangled and coherent states are not physically separated from their surroundings in a practical sense. Connecting such quantum systems to their surroundings results in a loss of coherence and entanglement due to dephasing effects [15]. This can be caused by a variety of factors in the environment, such as random particle mobility, thermal fluctuations, and various disorders, to name a few. Depending on the defect, the type of system, and the type of system–environment interaction involved, these faulty environments produce a variety of noises; for examples, see Refs. [16–20]. In this context, the local environmental

description is preferable because it allows for a more comprehensive investigation of quantum systems with multiple degrees of freedom. The coherence dynamics for decreasing degrading effects have been researched both theoretically and experimentally for a range of quantum systems under varied noisy situations [21–25].

We present a thorough investigation of the coherence preservation for a three-level system under various Gaussian noises. Among the noise types are fractional Gaussian noise ($\mathcal{FG}_n$), Gaussian noise ($\mathcal{G}_n$), Ornstein–Uhlenbeck noise ($\mathcal{OU}_n$), and power law noise ($\mathcal{PL}_n$). These noises are produced by the particles' usual random motions, which can degrade entanglement and coherence [26–28]. The study's primary aim will be to devise effective methods for preventing the deteriorating effects of the corresponding Gaussian noise. In addition, the comparative dynamics of coherence under various noises will be thoroughly investigated.

Non-Markovianity, local environment responses to coherence, entanglement protection, and statistical distinguishability on the density operator space, can be investigated using quantum Fisher information and quantum estimation theory, as discussed in [29,30]. The primary goal of the measurements is to determine the quantum Fisher information enhancement of open quantum systems so that unknown environmental parameters can be precisely measured. Important results have been achieved to prevent entanglement and coherence losses using quantum Fisher information and estimation theory for single and three-qubit states in [31–34]. In addition, in [35], coherence measurement has been investigated using entanglement-based coherence measures, distance-based coherence, and geometric coherence measures. In this paper, we look at the coherence preservation for a single qutrit state using two metrics: purity and von Neumann entropy [25]. To summarize the noise-free and noisy local fields' comprehensive coherence evaluation, besides purity and von Neumann entropy, we will be using the ℓ_1-norm of coherence [36].

The phase of a quantum system is crucial to the dynamics and symmetry of quantum systems and the associated transmitting channels. After computing the time-evolved density matrix, an average of the noise phases will be calculated to determine the noise's damaging effects. The quantum system's dynamics will be performed using the time unitary operation. Under the classical fluctuating field, the stochastic Hamiltonian is used to describe the energy state of the qutrit system. In both noisy and noise-free local environments, we examine the qualitative behavior of the system's coherence. The existence of a pure noiseless configuration is an ideal example; however, to decode a coherent state, it will be necessary to estimate the dissipation power and other local environmental characteristics. Differentiating between noiseless and noisy classical channels could help with quantum mechanical circuit design and long-term coherence preservation.

The major benefit of Gaussian processes is that they are tractable in many contexts and mimic a wide range of situations reasonably well. For example, in finance, Kalman filters, econometrics, satellite tracking, neural networks, machine learning, Bayesian reasoning, and other fields, Brownian motion and the related Gaussian noises are commonly used [37–42]. $\mathcal{FG}_n$, a stationary time series model with longer memory properties that have been applied in econometrics, hydrology, climatology, functional MRI, traffic networking and signaling, and so forth, could be part of the Gaussian process [43–47]. The Ornstein–Uhlenbeck process is stable, Gaussian, and Markovian; with Brownian motion-associated disorder causing $\mathcal{OU}_n$. This noise has been employed in studies including the intraday pairs trading strategy, stimulated Raman adiabatic passage systems, quantum control, modern quantum technologies, and other areas [48–51]. Furthermore, $\mathcal{PL}_n$ is another Gaussian noise used to model signal detection, human observer detection experiments, and surface growth and dynamics in lipid bilayers [52–55]. The dephasing effects generated by these Gaussian disturbances on the dynamical map of the three-level system in local external fields will be the focus of this paper. The purpose is to characterize the preservation of coherence and information encoded initially in the system over the complete range of the related noisy parameters. In this domain, workable methods for avoiding or minimizing Gaussian dephasing effects will be presented by utilizing the noise phase

via noise parameter adjustments. Therefore, this will lead to a longer preservation of quantum correlations. For example, by utilizing the parameters of bit-phase flip and the phase flip channels, quantum correlations have been shown to remain preserved in a noisy accelerated two-qubit system [56]. We also intend to provide computational values for the β-functions concerning various noise parameter values, which define the superimposed noise phase over the collective phase of the system and a classical fluctuating environment. This will lay the groundwork for the practical optimization of the classical fields with relative noise disorder.

The paper is organized as follows: In Section 2, the physical model and the associated dynamics of the three-level system in the classical fluctuating field under distinct noises will be presented. In Section 3, the results obtained are discussed. Section 4 will explain the conclusion from the present investigations.

2. Model and Dynamics

This section summarizes the required mathematical operations. We focus on the dynamical map of coherence in a three-level system that exists initially and which then evolves in classical fields of fluctuating nature driven by distinct Gaussian noises (see Figure 1). The Hamiltonian that governs the system's present dynamical map can be stated as [25]:

$$\mathcal{H}_{qt}(t) = \varepsilon I + \omega\eta(t)S_x, \tag{1}$$

where ε is the energy associated with the system. The qutrit's space is defined by the identity matrix I and the spin-1 operator S_x. ω is the qutrit-environment coupling strength, while $\eta(t)$ is the stochastic parameter that flips between ± 1, and its nature depends on the classical noise imposed on the external fields. Because of the random nature of the $\eta(t)$, the given Hamiltonian in Equation (1) is stochastic and explains the stochastic dynamics of the three-level system with time. The corresponding time evolution operation for the three-level system can be written as [57]:

$$\mathcal{U}_{qt}(t) = \exp\left[-i\int_0^t \mathcal{H}_{qt}(s)ds\right], \tag{2}$$

where $\hbar = 1$. If the qutrit system is initially prepared in the state ρ_o, then the time-evolved density matrix can be expressed in the following form as [57]:

$$\rho_{qt}(t) = \mathcal{U}_{qt}(t)\rho_o U_{qt}(t)^{\dagger}. \tag{3}$$

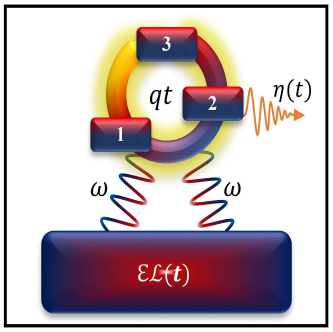

Figure 1. The current configuration model depicts the coupling of a three-level system qt exposed to a classical fluctuation field $\mathcal{EL}(t)$. The system–environment coupling strength ω is shown by the blue-reddish wavy lines, while the noise's influence is represented by the yellowish light in the qutrit. The brownish-wavy lines depict system dynamics as defined by the associated environment's stochastic parameter $\eta(t)$, with diminishing amplitude showing Gaussian noise-induced dephasing.

2.1. Impact of Local Gaussian Noises

Various local Gaussian noises are defined here to include the noisy effects. In this proceeding, we evaluate the application of the fractional Gaussian ($\mathcal{FG}_n$), Gaussian ($\mathcal{G}_n$), Ornstein–Uhlenbeck ($\mathcal{OU}_n$), and power law noise ($\mathcal{PL}_n$). The random mobility of the particles in the diffusion process causes $\mathcal{FG}_n$ and $\mathcal{OU}_n$. This can disrupt the dynamics of quantum systems, necessitating further investigation. Because of its larger timescale correlations, $\mathcal{FG}_n$ has been utilized to analyze meteorological information [58], traffic control analysis [59], and electrical measurements [60]. The $\mathcal{OU}_n$ has been extensively studied with the dynamics of quantum systems, as described in [57]. Similarly, the discrete nature of warm object radiation causes $\mathcal{G}_n$ and gives rise to the thermal vibration of the medium's particle, and is used to study digital imaging [61], signal detection, and phase transitions [62]. Finally, in solid-state and superconducting materials, the $\mathcal{PL}_n$ is a low-frequency noise caused by resistance. This noise has been already studied for the scaling of surface fluctuations and the dynamics of surface growth models [63], human-observed detection experiments with mammograms [53], and the discrete simulation of colored noise and stochastic processes [64].

To impose classical noise over the time evolution of the system, one has to include the β-function, which reads as [57]:

$$\beta(t) = \int_0^t \int_0^t K(s - s')dsds'. \tag{4}$$

We look at four different Gaussian processes. To be more specific, we suppose that the stochastic field $\beta(t)$ is driven by $\mathcal{FG}_n$, $\mathcal{OU}_n$, $\mathcal{G}_n$, or $\mathcal{PL}_n$. The associated autocorrelation function of $\mathcal{FG}_n$ with a diffusion coefficient which proportionally grows as τ^{2H} can be written as [28,57]:

$$K_{\mathcal{FG}_n}(\tau - \tau') = \frac{|\tau'|^{2H} - |\tau - \tau'|^{2H} + |\tau|^{2H}}{2}. \tag{5}$$

where $0 \leq H \leq 1$ is known as the Hurst index (H). This autocorrelation function is specifically defined for three different values. When $H = \frac{1}{2}$, the effects of $\mathcal{FG}_n$ noise become similar to the Wiener process. At $H < \frac{1}{2}$, Equation (5) enters a sub-diffusive process and the increments of the expressions are negatively correlated. When $H > \frac{1}{2}$, the autocorrelation function of the noise reaches the super-diffusive regime and the related increments of the equation become positive. The β-function for the $\mathcal{FG}_n$ can be obtained by inserting the autocorrelation function from Equation (5) into Equation (4) as in [57]:

$$\beta_{\mathcal{FG}_n}(\tau) = \frac{\tau^{2(H+1)}}{2(H+1)}. \tag{6}$$

In the case of $\mathcal{G}_n$, $\mathcal{OU}_n$, and $\mathcal{PL}_n$, the corresponding autocorrelation expressions are:

$$K_{\mathcal{G}_n}(t - t', \gamma, \Gamma) = \frac{\Gamma\gamma \exp[-\gamma^2(t - t')^2]}{\sqrt{\pi}}, \tag{7}$$

$$K_{\mathcal{OU}_n}(t - t', \gamma, \Gamma) = \frac{\gamma\Gamma \exp[-\gamma|t - t'|]}{2}, \tag{8}$$

$$K_{\mathcal{PL}_n}(t - t', \gamma, \Gamma, \alpha) = \frac{[\alpha - 1]\chi\Gamma}{2[\chi|t - t'| + 1]^2}, \tag{9}$$

where Γ regulates the damping rate and α is the unknown parameter in the case of $\mathcal{PL}_n$, which has been also demonstrated to carry noisy detrimental effects. For the $\mathcal{G}_n$, we assume

$g = \frac{\gamma}{\Gamma}$ and $\tau = \Gamma t$, where γ is also a dephasing Gaussian noise parameter. By inserting the autocorrelation function from Equation (7) into Equation (4), we obtain [28]:

$$\beta_{\mathcal{G}_{\mathcal{N}}}(\tau) = \frac{1}{g}\left[\frac{e^{-g^2\tau^2} - 1}{\sqrt{\pi}} + \mathrm{Erf}[g\tau](g\tau)\right], \tag{10}$$

where $\mathrm{Erf}[g\tau] = \frac{2}{\sqrt{\pi}}\int_0^{g\tau} \exp[-t^2]dt$ is the error function of the normalized Gaussian distribution. The relative β-function for the $\mathcal{OU}_n$ can be obtained by inserting Equation (8) into Equation (4) and can be expressed in the form [57]:

$$\beta_{\mathcal{OU}_n}(\tau) = \frac{g\tau + \exp[-g\tau] - 1}{g}, \tag{11}$$

where g is the inverse of the autocorrelation time τ. Similarly, for $\mathcal{PL}_n$, we recall $g = \frac{\gamma}{\Gamma}$ and $\tau = \Gamma t$ and insert the autocorrelation function given in Equation (9) into Equation (4); we obtain the β-function as in [28]:

$$\beta_{\mathcal{PL}_n}(\tau) = \frac{g\tau(\alpha - 2) - 1 + (1 + g\tau)^{2-\alpha}}{g(\alpha - 2)}. \tag{12}$$

The final density matrix of the system is averaged over the random phase factor ϕ as $\langle e^{\pm n\phi(t)}\rangle = \langle e^{\theta(\tau)}\rangle$, where $\phi = in\omega\eta(t)$, with $n \in \mathbb{N}$ being the phase factor determining the dynamical characteristic of the system in the local random fields, and $\theta(\tau) = -\frac{1}{2}n^2\beta_{\mathcal{AB}}(\tau)$ (with $\mathcal{AB} \in \{\mathcal{FG}_n, \mathcal{G}_n, \mathcal{OU}_n, \mathcal{PL}_n\}$) is the phase factor of the local Gaussian noise. The time-evolved density matrix of the system can be obtained using [57]:

$$\rho_{qt}(\tau) = \left\langle U_{qt}(t)\rho_o U_{qt}^{\dagger}(t)\right\rangle_{\theta(\tau)}. \tag{13}$$

2.2. Coherence Measures

The degree of mixedness of a quantum state, or the coherence of a pure initial state that reflects the physical system because of interactions with classical environments, is determined according to purity. For a quantum state $\rho_{qt}(\tau)$, purity can be determined by [25]:

$$\mathcal{P}_r(\tau) = \mathrm{Tr}\left[\rho_{qt}^2(\tau)\right], \tag{14}$$

where for a system of n-dimensions, the purity ranges as: $\frac{1}{n} \leq \mathcal{P}_r(\tau) \leq 1$. The state of being pure and coherent occurs at $\mathcal{P}_r(\tau) = 1$, while it is entirely mixed and decoherent at $\frac{1}{n}$.

Decoherence occurs when quantum systems' wave functions interact with their coupled environments. As a result, rather than being a single coherent quantum superposition, the system behaves similarly to a classical statistical ensemble of its constituents. The decoherence phenomenon will be a credible measure to calculate the coherence loss in the time-evolved state of the system, because the system–environment interaction is depicted classically here. The von Neumann entropy technique can assess the decoherence effects for the time-evolving density matrix as [25]:

$$\mathcal{V}_e(\tau) = -\mathrm{Tr}\left[\rho_{qt}(\tau)\log\rho_{qt}(\tau)\right]. \tag{15}$$

$\mathcal{V}_e(\tau) = 0$ indicates that the state is coherent with no information loss. Any other value will represent the corresponding amount of coherence and information loss for the three-level system.

3. Main Results

In this part, we provide the major findings for the dynamics of a qutrit system under Gaussian noise emanating from a classical fluctuating field. Apart from that, the results of Equations (14) and (15) will be analyzed to see how purity and von Neumann entropy have changed over time. In order to determine the current noise's ability to dephase the single qutrit system, the system's dynamics are explored in both noiseless and noisy conditions.

3.1. The Noiseless Classical Field

The dynamics of the single qutrit system, when subjected to a noise-free stochastic field, is discussed in this section. Using the existing dynamical setup of the system in a noise-free context, the original role of stochastic fields in noise exclusion can be demonstrated. This will also discriminate between the qualitative dynamical map of a single qutrit system in both noiseless and noisy classical fields. The following is the time unitary operation matrix:

$$\mathcal{U}_{qt}(t) = \exp(-it\epsilon)\begin{bmatrix} \cos\left[\frac{\phi}{2}\right]^2 & -\frac{i\sin[\phi]}{\sqrt{2}} & \frac{1}{2}(-1+\cos[\phi]) \\ -\frac{i\sin[\phi]}{\sqrt{2}} & \cos[\phi] & -\frac{i\sin[\phi]}{\sqrt{2}} \\ \frac{1}{2}(-1+\cos[\phi]) & -\frac{i\sin[\phi]}{\sqrt{2}} & \cos\left[\frac{\phi}{2}\right]^2 \end{bmatrix}, \tag{16}$$

while the initial density matrix is considered in the form $\rho_o = |\psi\rangle\langle\psi|$, $\psi = \frac{1}{\sqrt{3}}(|0\rangle + |1\rangle + |2\rangle)$. The final density matrix, computed using Equation (3), can be put into the following form:

$$\rho_{qt}(t) = \frac{1}{12}\begin{bmatrix} 3+\cos[2\phi] & 4+i\sqrt{2}\sin[2\phi] & 3+\cos[2\phi] \\ 4-i\sqrt{2}\sin[2\phi] & 6-2\cos[2\phi] & 4-i\sqrt{2}\sin[2\phi] \\ 3+\cos[2\phi] & 4+i\sqrt{2}\sin[2\phi] & 3+\cos[2\phi] \end{bmatrix}. \tag{17}$$

The structure of the density matrix given in Equation (17) illustrates that the system is coherent, as the off-diagonal elements of the matrix are non-zero. Furthermore, for the density matrix $\mathcal{P}_r(t) = 1$ and $\mathcal{V}_e(t) = 0$, the system is hence portrayed to be coherent.

To analyze the coherence qualitative dynamical map for the time-evolved density matrix of the system given in Equation (17), we use the ℓ_1-norm of coherence, which can be computed as [36]:

$$C(t) = \sum_{i\neq j} |\langle i|\rho_{qt}(t)|j\rangle|, \tag{18}$$

where $\sum_{i\neq j}|.|$ is the sum of the absolute values of the off-diagonal elements of $\rho_{qt}(t)$ in the chosen reference basis. It is worth mentioning that the ℓ_1-norm of coherence has a range of $0 \leq C(t) \leq n-1$, where n are the dimensions of the system [65]. Therefore, for the current qutrit system, the ℓ_1-norm of coherence will range as $0 \leq C(t) \leq 2$.

Figure 2 shows the dynamics of coherence for the time-evolved density matrix state given in Equation (3) for the single qutrit system when coupled to the classical field against coupling strength ω and classical stochastic parameter η. Note that the superposition of the noise phase over the system phase is not applied. From the current results, we find that such local environments have a random character and strongly support coherence revivals. These fluctuations are the main reasons for the dynamics and preservation of coherence. As in most of the previous results, whenever the revival character in the dynamical maps of the system vanishes, the coherent states become decoherent; for example, see the Refs. [57,66–69]. Thus, the fluctuating character of the current local channels influenced by disorders can be helpful for preserving the coherence encoded initially in a quantum state. Here, the fluctuation rate in coherence is influenced by the qutrit-environment coupling strength ω and the stochastic parameter η of the classical field. One can note that the number of revivals is greater for the increasing strength of ω in Figure 2a and for η in

Figure 2b. In agreement, the stochastic parameter also influences the revival frequency of coherence, as for the increasing η values, the ℓ_1-norm of coherence faces a repeated and increasing number of oscillations. The amplitude of the fluctuations is completely independent of the ω as well as of $\eta(t)$, and only depends upon the type of system involved. This optimal setting for controlling the revivals of coherence can lead to the engineering and design of circuits and protocols for the required results [70–72]. We conclude that the three-level system remains a resource state in the noise-free classical fields, exhibiting a dynamical map with no coherence loss, and that it does not transition from the resource state to the free state regime completely.

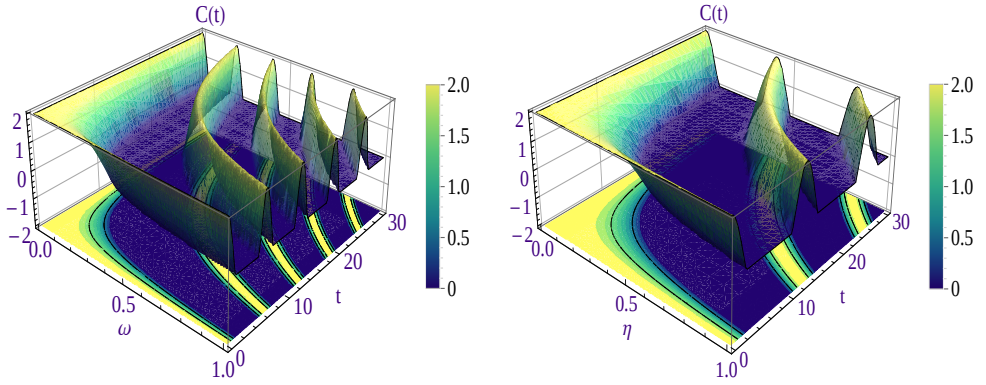

(**a**) (**b**)

Figure 2. Time evolution of coherence in a single qutrit system prepared in the time-evolved state $\rho_{qt}(t)$ given in Equation (19) subjected to a noiseless classical channel when (**a**) $\eta = 1, 0 \leq \omega \leq 1$ and (**b**) $0 \leq \eta \leq 1, \omega = 0.5$ against the time evolution parameter t.

3.2. A Classical Field with Gaussian Noises

The application of Gaussian noises to the time-evolved density matrix of the single qutrit system described in Equation (13) is covered in this section. In the current case, the noise phase is superimposed over the system's phase. The final density matrix for the three-level system under the Gaussian noise computed has the form:

$$\rho_{qt}^{\mathcal{AB}_n}(\tau) = \begin{bmatrix} \frac{1}{12}(3+\mathcal{M}_{\mathcal{AB}_n}) & \frac{1}{3} & \frac{1}{12}(3+\mathcal{M}_{\mathcal{AB}_n}) \\ \frac{1}{3} & \frac{1}{2}-\frac{\mathcal{M}_{\mathcal{AB}_n}}{6} & \frac{1}{3} \\ \frac{1}{12}(3+\mathcal{M}_{\mathcal{AB}_n}) & \frac{1}{3} & \frac{1}{12}(3+\mathcal{M}_{\mathcal{AB}_n}) \end{bmatrix}, \tag{19}$$

where

$$\rho_{qt}^{\mathcal{AB}_n}(\tau) \in \{\rho_{qt}^{\mathcal{FG}_n}(\tau), \rho_{qt}^{\mathcal{G}_n}(\tau), \rho_{qt}^{\mathcal{OU}_n}(\tau), \rho_{qt}^{\mathcal{PL}_n}(\tau)\}, \quad \mathcal{M}_{\mathcal{AB}_n} \in \{\mathcal{M}_{\mathcal{FG}_n}, \mathcal{M}_{\mathcal{G}_n}, \mathcal{M}_{\mathcal{OU}_n}, \mathcal{M}_{\mathcal{PL}_n}\},$$

with

$$\mathcal{M}_{\mathcal{FG}_n} = e^{-\frac{\tau^{2H+2}}{H+1}}, \qquad \mathcal{M}_{\mathcal{G}_n} = \exp\left[-\frac{2\left((g\tau)\mathrm{erf}(g\tau) + \frac{e^{-g^2\tau^2}-1}{\sqrt{\pi}}\right)}{g}\right],$$

$$\mathcal{M}_{\mathcal{OU}_n} = e^{-\frac{2\left(g\tau+e^{-g\tau}-1\right)}{g}}, \qquad \mathcal{M}_{\mathcal{PL}_n} = \exp\left[-\frac{2\left((g\tau+1)^{2-\alpha}+(\alpha-2)g\tau-1\right)}{(\alpha-2)g}\right].$$

Under the effects of Gaussian noises, the diagonal and off-diagonal components of the aforementioned matrix differ from those in Equation (17), but they do not vanish. Therefore, the current three-level state remained coherent, even under the presence of noise. This means the single three-level system is a better resource in terms of informa-

tion preservation than bipartite and tripartite quantum systems, which suffer from more loss [16–20,66,68,73–76].

Using Equation (18) for the final density matrix given in Equation (19), the result obtained for ℓ_1-norm of coherence has the following form:

$$C(\tau) = \frac{1}{6}(|3 + \mathcal{M}_{\mathcal{AB}_n}| + 8). \tag{20}$$

In Figure 3, the dynamics of the coherence in the final density matrix of the single qutrit system under local Gaussian noises originating from the stochastic field is depicted. The current results reflect the time evolution of the coherence when the noise phases is superimposed on the system phase. By comparing Figures 2 and 3, one may easily determine the prevailing deteriorating character of classical noises for coherence and the revival character of the local fields. Because of the Gaussian noisy classical field, the fluctuations are eradicated after the first death. This means that the coherence revivals seen in noise-free classical fields were completely dampened in the dynamical map of the three-level system under Gaussian noises. Therefore, this demonstrates that information transmission between the qutrit and its environment is not supported, and that information loss is irreversible. When subjected to the classical fields regulated by the Gaussian noises, the interconversion of the free and resource three-level system is completely restricted. This implies that quantum information processing involving local Gaussian noisy fields will be a delicate operation with a high risk of failure. As shown in [66,68], this characteristic has also been proven in quantum correlations and in the survival of coherence in classical fields with non-Gaussian noises, causing total or partial non-local correlation losses. Each noise, as well as its associated parameters, has a different ability to suppress coherence throughout time. In the specified Hurst exponent (H) range, the decay is substantially higher and faster. When compared to $\mathcal{FG}_n$, the relative losses in the cases of $\mathcal{G}_n$, $\mathcal{OU}_n$, and $\mathcal{PL}_n$ are significantly reduced for both the high and low values of the noisy parameters. It is worth noting that the decay behavior of $\mathcal{FG}_n$ differs significantly from that of other existing noises and that there is no evidence of a significant rise in decay when the parameter H is increased. This is in direct contrast to the latter included noises when the slopes change towards higher decay as the noisy parameters are increased. The decay caused by the $\mathcal{PL}_n$ seems to be similar to that of $\mathcal{FG}_n$; however, the intrinsic roles of their corresponding parameters α and H seem to be the opposite. Furthermore, $\mathcal{FG}_n$ is followed by $\mathcal{PL}_n$ in producing greater dephasing effects. As in the cases of $\mathcal{G}_n$ and $\mathcal{OU}_n$ noises, when g approaches zero, the initial coherence remains preserved for indefinite intervals. The saturation values for all the included noises remained constant, implying a comparable relevant Gaussian character. Based on the existing findings, it is possible to predict that the non-local correlations and information decay caused by these noises will be monotonic rather than having revivals.

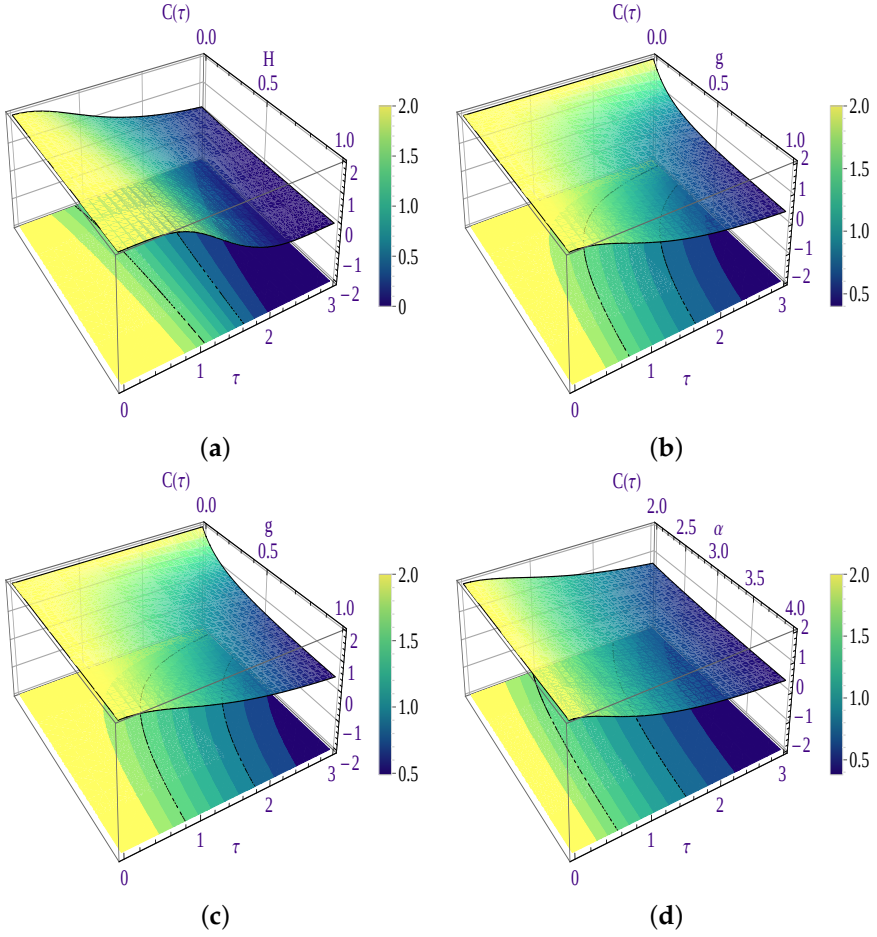

Figure 3. Time evolution of coherence in a single qutrit system prepared in the time-evolved state $\rho_{qt}(\tau)$ given in Equation (19) when subjected to the classical field generating (**a**) fractional Gaussian noise when $0 \leq H \leq 1$ and (**b**) Gaussian noise when $0 \leq g \leq 1$, (**c**) Ornstein–Uhlenbeck noise when $0 \leq g \leq 1$ and (**d**) power law noise when $2 \leq \alpha \leq 4$ with $g = 1$ against evolution parameter $\tau = 3$.

3.2.1. A Classical Field with $\mathcal{FG}_n$

The dynamics of the single qutrit system originating from the classical field under $\mathcal{FG}_n$ is briefly investigated here. The impact of current noise is applied by averaging the final density matrix in Equation (13) over the noisy phase with the β-function from Equation (6). In Equation (19), we find that the diagonal- and off-diagonal terms are non-vanishing. This means the qutrit system is still coherent under $\mathcal{FG}_n$. The density matrix states calculated for many quantum systems studied in [57] contradict this, where many elements of the final density matrix of the systems vanished, resulting in larger or complete decoherence. The following analytical results are obtained using Equations (14) and (15) for the system's final density matrix:

$$\mathcal{P}_r(\tau) = \frac{1}{18}\left(17 + \cosh[\frac{2(\tau^2)^{1+H}\cos[2(1+H)\mathrm{Arg}[\tau]]}{1+H}] - \sin[\frac{2(\tau^2)^{1+H}\cos[2(1+H)\mathrm{Arg}[\tau]]}{1+H}]\right), \tag{21}$$

$$\begin{aligned}\mathcal{V}_e(\tau) =& \frac{1}{6}\nu_1\left(-3\nu_2 + \sqrt{\nu_2 + 8\nu_3}\right)\log[\frac{1}{6}(3 - \nu_1\sqrt{\nu_2 + 8\nu_3}]\right) \\ &-\frac{1}{6}\nu_1\left(3\nu_2 + \sqrt{\nu_2 + 8\nu_3}\right)\log[\frac{1}{6}(3 + \nu_1\sqrt{\nu_2 + 8\nu_3}]\right),\end{aligned} \tag{22}$$

where

$$\nu_1 = e^{-\frac{2\tau^{2+2H}}{1+H}}, \qquad \nu_2 = e^{\frac{2\tau^{2+2H}}{1+H}},$$
$$\nu_3 = e^{\frac{4\tau^{2+2H}}{1+H}}.$$

Figure 4 explores the dynamics of the purity and von Neumann entropy for a single qutrit system under the local $\mathcal{FG}_n$. By comparing Figures 2–4, the destructive nature of the $\mathcal{FG}_n$ towards the revivals and preservation of the coherence and information is obvious enough. Purity and coherence, because of $\mathcal{FG}_n$, attain final saturation values after undergoing maximum decay. It is important to recall that the present saturation levels only reflect a small partial loss of coherence and information. This is both startling and counterintuitive to most previous results for systems with multiple qubits or qutrits [57,67,68], where a greater loss of information has been observed. This means that once the information is lost, then this noise does not facilitate the repeated interchange of information between the system and the environment. One might deduce that the information degradation is irreversible and cannot be reversed, as also shown in [57,77–80], where a temporary reversible decay occurred. The dynamics of the bipartite and tripartite states under $\mathcal{OU}_n$, and pure and mixed Gaussian noises have the same monotonic qualitative decay; through with different decay levels or reaching complete separability [57,77–80]. We find it distinct that, for increasing choices of H, the slopes shift from the green to the red end. This implies the supporting nature of the parameter H for memory properties of the environments, and the opposite results have been obtained while discussing different noise parameters, such as in [57,67,77,78] where decay increases with the increase in the noisy parameters. All of the parameter values overlap at the peaks and minima, indicating that both measures suggest a single saturation level, and therefore they predict a good agreement between them. The current noise parameters do not affect the loss in this case, but the noise phase has an enormous impact. Adjusting the parameters has only a minor impact on the preservation duration, and any choice of H does not guarantee that the coherence and information will be preserved. Because of the discrete nature, we found no ultimate solution or ideal parameter fixing to avoid the $\mathcal{FG}_n$ noisy detrimental effects. Avoiding classical environments with discrete Brownian motions of the relative constituents is the only method to reduce this type of noise. The β-function for $H = \{0.1, 0.5, 0.9\}$ is computed to be $\beta = \{2.08854, 2.66667, 3.66548\}$. Within classical environments with $\mathcal{FG}_n$ disorders, these precise values will be useful in optimizing quantum correlations and the coherence survival time.

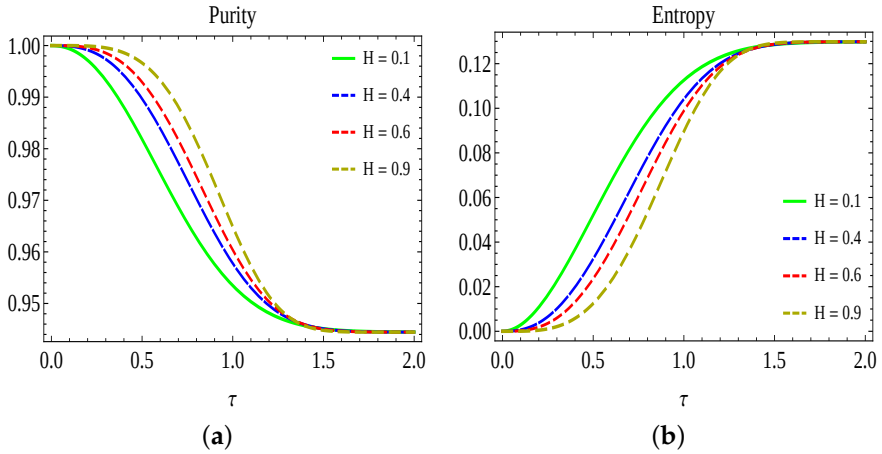

Figure 4. Time evolution of (**a**) purity and (**b**) von Neumann entropy as functions of H versus τ in a single qutrit system when subjected to the classical field generating fractional Gaussian noise.

3.2.2. A Classical Field with $\mathcal{G}_n$

Performing the average of the final density matrix given in Equation (13) over the noise phase with the β-function given in Equation (10) results in the dynamics of the single qutrit system under $\mathcal{G}_n$. From the final density matrix given in Equation (19), it is readily deducible that the system remains coherent under the current noisy configuration because of the non-vanishing terms.

In contrast, the bipartite and tripartite states given in [16–20,57] remained more fragile to the local noisy environments and became less coherent shortly, as compared to the current three-level system. From Equations (14) and (15), the analytical results for the current configuration are:

$$\mathcal{P}_r(\tau) = \frac{1}{18}\left(17 + e^{\frac{4\left(1-e^{-g^2\tau^2}\right)}{\sqrt{\pi}} - 4g\tau \mathrm{Erf}[g\tau]}{g}\right), \tag{23}$$

$$\mathcal{V}_e(\tau) = \eta_1\left((-3\eta_2 + \sqrt{\eta_3})\log\left[\frac{1}{6}(3 - \eta_1\sqrt{\eta_3})\right] - (3\eta_4 + \sqrt{\eta_3})\log\left[\frac{1}{6}(3 + \eta_2\sqrt{\eta_3})\right]\right), \tag{24}$$

where

$$\eta_1 = \frac{1}{6}e^{-\frac{4e^{-g^2\tau^2}}{g\sqrt{\pi}} - 4\tau\mathrm{Erf}[g\tau]}, \qquad \eta_2 = e^{\frac{4e^{-g^2\tau^2}}{g\sqrt{\pi}} + 4\tau\mathrm{Erf}[g\tau]},$$

$$\eta_3 = 8e^{\frac{8e^{-g^2\tau^2}}{g\sqrt{\pi}} + 8\tau\mathrm{Erf}[g\tau]} + e^{\frac{4\left(\frac{1+e^{-g^2\tau^2}}{\sqrt{\pi}} + g\tau\mathrm{Erf}[g\tau]\right)}{g}}, \qquad \eta_4 = e^{-\frac{4e^{-g^2\tau^2}}{g\sqrt{\pi}} - 4\tau\mathrm{Erf}[g\tau]}.$$

Figure 5 shows the dynamics of purity and von Neumann entropy for a single qutrit system when subjected to the classical field with $\mathcal{G}_n$. The system's time evolution is investigated further for various g values against τ. By comparing Figures 2, 3 and 5, one can deduce the dominating deteriorating character of the $\mathcal{G}_n$ to the lower preservation capacities and vanishing revival features of the environments. Due to $\mathcal{G}_n$, the initially encoded purity and coherence in the system showed a monotonic decline rather than showing any rebirths. As a result, the classical random field with $\mathcal{G}_n$ does not allow information from the environment to flow back into the system. One can deduce that the degradation produced by $\mathcal{G}_n$ is irreversible. The observed qualitative behaviors for bipartite and tripartite states are consistent with the previous results obtained under various kinds of Gaussian noises studied in [57,77–80]. However, the related quantitative analysis has many differences, such as a greater loss and preservation time. When g increases, the slopes move from the green to the red end. For large values of g, this means a higher occurrence of purity and coherence loss. Due to $\mathcal{FG}_n$, the decay encountered is incompatible with this behavior. It is important to note that under $\mathcal{G}_n$, the coherence and information are not lost entirely and they reach a final saturation level after maximal decay. This property of the single qutrit system, which shows a minimal partial loss rather than a complete loss, is a useful resource that contradicts most of the previous findings obtained for bipartite and tripartite qubit systems in [57,66,76–80], where the quantum systems become easily decoherent. According to both measures, the saturation levels for each value of the noise parameter meet at the same height, implying that the decay levels are the same. The measures' maxima and minima are comparable, showing that the results are consistent. In addition, the $\mathcal{G}_n$ noise phase is less decoherent towards the coherence and information decay than the $\mathcal{FG}_n$ noise phase. Unlike the $\mathcal{FG}_n$, the $\mathcal{G}_n$ exhibits flexible noise parameter range values. This makes it easier to characterize the classical environments with $\mathcal{G}_n$ for optimal longer quantum correlations and coherence preservation times. For $g = \{1, 3, 10\}$, the corresponding β-functions for the current noise have the values of $\beta = \{1.43679, 1.81194, 1.94358\}$.

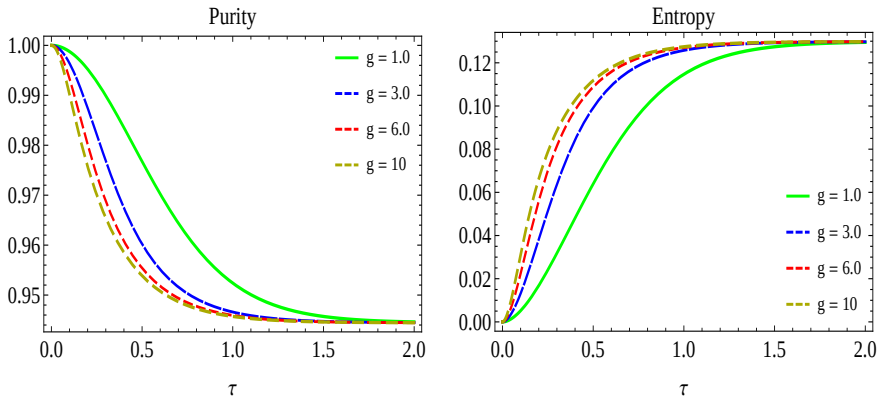

Figure 5. Time evolution of (**a**) purity and (**b**) von Neumann entropy as functions of H versus τ in a single qutrit system when subjected to the classical field generating Gaussian noise.

3.2.3. A Classical Field with $\mathcal{OU}_n$

This section involves the noisy effects due to $\mathcal{OU}_n$ by averaging the final density matrix given in Equation (13) over the noise phase having the β-function from Equation (11). The final density matrix obtained for the three-level system under $\mathcal{OU}_n$ agrees with those obtained under the $\mathcal{FG}_n$ and $\mathcal{G}_n$ and shows that the system remains coherent.

The analytical results for the $\mathcal{P}_r(\tau)$ and $\mathcal{V}_e(\tau)$ are obtained from Equations (14) and (15) and are followed as:

$$\mathcal{P}_r(\tau) = \frac{1}{18}\left(17 + e^{\frac{4-4e^{-g\tau}-4g\tau}{g}}\right), \tag{25}$$

$$\mathcal{V}_e(\tau) = -\frac{3-\gamma_1}{6}\log\left[\frac{3-\gamma_1}{6}\right] - \frac{3+\gamma_1}{6}\log\left[\frac{3+\gamma_1}{6}\right], \tag{26}$$

where

$$\gamma_1 = e^{-\frac{4e^{-g\tau}}{g}-4\tau}\sqrt{e^{\frac{4}{g}+\frac{4e^{-g\tau}}{g}+4\tau} + 8e^{\frac{8e^{-g\tau}}{g}+8\tau}},$$

Figure 6 shows the dynamics of the purity and von Neumann entropy for the single qutrit system when coupled to the classical field generating $\mathcal{OU}_n$. The degrading quality of the $\mathcal{OU}_n$ is shown by comparing the initial purity and coherence with the latter. The loss caused by the current noise has resulted in monotonous functions over time with no revivals. The current monotonic decay under $\mathcal{OU}_n$ contradicts the findings of bipartite and hybrid qubit-qutrit state dynamics given in [57,67], where evident revivals of coherence have been detected. The initial encoded purity, coherence, and information are not fully lost, and the saturation threshold is reached. The measures' maximum and minimum values are comparable, and there is a single saturation level for all g values. By comparing Figures 2, 3 and 6, it is easy to determine that this noise has a dominant character to suppress oscillation and the preservation capacity of the system. We noticed that as compared to the previously investigated systems in [77,79–82], the single qutrit system exhibited a superior preservation capacity. Aside from that, raising the noise parameter g caused the initial encoded purity, coherence, and information to decay faster. As seen, the slopes move towards the red end with increasing values of g, suggesting greater degradation. However, by limiting g to be as minimal as possible, the optimal smaller decay can be produced. In contrast to $\mathcal{FG}_n$, the present noise phase has shown to have a lower deteriorating character for the memory properties of the system, as the preservation time encountered in the current case is longer. Similar to the $\mathcal{G}_n$, the $\mathcal{OU}_n$ has the same large range in terms of g. The dephasing effects because of the superposition of the $\mathcal{OU}_n$ over the system's phase are

lesser than those of the $\mathcal{FG}n$. This is owing to $\mathcal{OU}_n$'s exploitable noise phase, which was not possible in the case of $\mathcal{FG}_n$. With $g = \{1, 3, 10\}$, the corresponding β-function amounts as $\beta = \{1.13534, 1.66749, 1.9\}$.

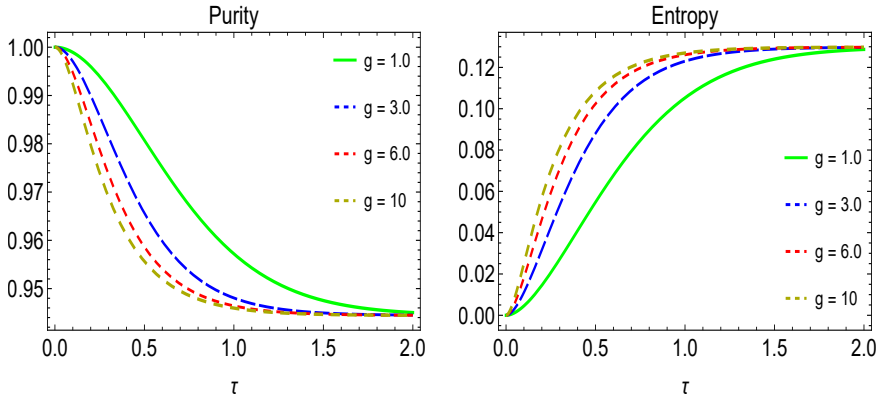

Figure 6. Time evolution of (**a**) purity and (**b**) von Neumann entropy as functions of H versus τ in a single qutrit system when subjected to the classical field generating Ornstein–Uhlenbeck noise.

3.2.4. A Classical Field with $\mathcal{PL}_n$

To evaluate the degrading effects of the $\mathcal{PL}_n$ over the dynamics of the single qutrit state, we perform an average of the final density matrix given in Equation (13) over the noise phase with the β-function given in Equation (12). The structure of the final density matrix under the current noise ensures that the three-level system does not become entirely decoherent. By using the Equations (14) and (15), the corresponding analytical results for the $\mathcal{P}_r(\tau)$ and $\mathcal{V}_e(\tau)$ are followed as:

$$\mathcal{P}_r(\tau) = \frac{1}{18}\left(17 + e^{4\delta_1 - 4\tau - \frac{4((1+g\tau)^2)^{1-\frac{\alpha}{2}}\cos[(-2+\alpha)\mathrm{Arg}[1+g\tau]]}{g(-2+\alpha)}}\right), \tag{27}$$

$$\begin{aligned}\mathcal{V}_e(\tau) = &-\frac{1}{6}\left(3 - e^{-4\delta_2}\sqrt{8e^{8\delta_2} + e^{4(\delta_2+\delta_1)}}\right)\log\left[\frac{1}{6}\left(3 - e^{-4\delta_2}\sqrt{8e^{8\delta_2} + e^{4(\delta_2+\delta_1)}}\right)\right] \\ &-\frac{1}{6}\left(3 + e^{-4\delta_2}\sqrt{8e^{8\delta_2} + e^{4(\delta_2+\xi_1)}}\right)\log\left[\frac{1}{6}\left(3 + e^{-4\delta_2}\sqrt{8e^{8\delta_2} + e^{4(\delta_2+\delta_1)}}\right)\right],\end{aligned} \tag{28}$$

where

$$\delta_1 = \frac{1}{g(-2+\alpha)}, \qquad \delta_2 = \tau + \frac{(1+g\tau)^{2-\alpha}}{g(-2+\alpha)}.$$

Figure 7 shows the time evolution of the purity and von Neumann entropy for the single qutrit system when subjected to a classical random field with $\mathcal{PL}_n$. In the current case, the dynamics of the system are investigated under two different noisy parameters, namely g (upper panel) and α (bottom panel). By comparing Figures 2, 3 and 7, the dissipative capability of the $\mathcal{PL}_n$ in terms of the capability of two noisy parameters to disappear revivals and to lower the initial encoded coherence and information can be validated. Large values of g have greater degraded purity, coherence, and information than the parameter α. For g, the slopes for purity and von Neumann entropy reach saturation values faster than for α. Aside from the decaying nature of the $\mathcal{PL}_n$, the smaller partial loss rather than complete decay cannot be overlooked. This directly opposes most of the prior findings for various quantum systems, where in most cases, complete separability is reached, as discussed in [57,77–81,83,84]. All of the slopes for various noise parameter values reach a single saturation level, although at different intervals. As a result, there appears to be a strong link between the measures for demonstrating consistency and agreement in the

results. As the values of both parameters increase, the slopes move from the green to the red end, implying that the decay rate increases. In the current cases, this qualitative behavior is comparable to those of the $\mathcal{OU}_n$ and mixed Gaussian noise; nevertheless, the decay levels encountered for the single qutrit system differ significantly from those previously investigated [57,77,80]. There was no evidence of revivals in the dynamical map of the system, and both noisy parameters showed a monotonic decline in coherence. As a result, there is no way for information from the environment to flow back into the system, contradicting the findings in [67,85,86], where a strong backflow of the information into the system has been observed. Because of this noise, purity, coherence, and information are permanently lost rather than experiencing periodic transitory deterioration. In the case of $\mathcal{PL}_n$, the β-function is characterized by two noisy parameters, g and α. With $\alpha = 3$, the β-function ranges as $\beta = \{1.333, 1.71429, 1.90476\}$ for $g = \{1, 3, 10\}$. By keeping $g = 0.5$ and $\alpha = \{3, 5, 10\}$, the relative β-function has values as $\beta = \{1.0, 1.41667, 1.75098\}$.

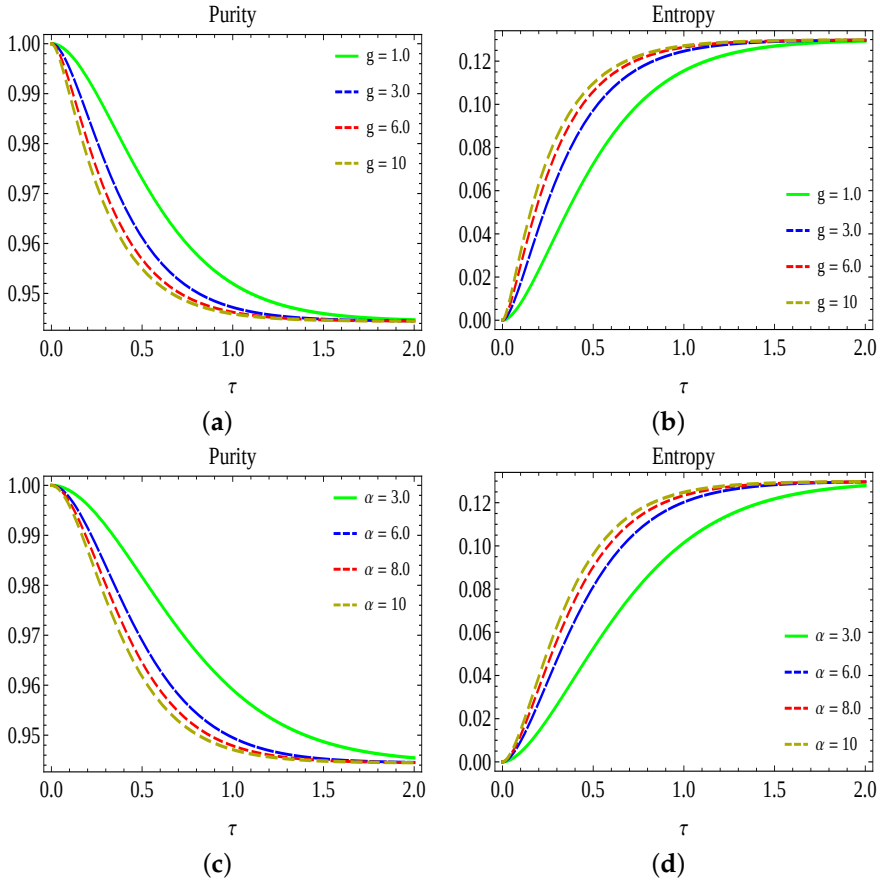

Figure 7. Upper Panel: Time evolution of (**a**) purity and (**b**) von Neumann entropy as functions of g versus τ in a single qutrit system when subjected to the classical field generating power law noise when $\alpha = 3$. Bottom panel: Time evolution of (**c**) purity and (**d**) von Neumann entropy as functions of α versus τ in a single qutrit system when subjected to the classical field generating power law noise when $g = 0.5$.

3.3. Relative Dynamics

The present section explains the comparative dynamical map of the coherence and information encoded in the system under the present Gaussian noises. Here, we intend to provide the adjustment of the noise parameters to reduce the dephasing effects and to increase the coherence span time. For this purpose, we assumed the noise parameters at the lowest and highest values of the corresponding range.

Figure 8 evaluates the time evolution of the purity (a) and von Neumann entropy (b) for the single qutrit system under the presence of $\mathcal{G}_n$ in the green, $\mathcal{OU}_n$ in the blue, and $\mathcal{PL}_n$ in

the red slopes. We mainly focus on protecting purity, coherence, and information for a large duration. Following this, we have set the noise parameter $g = 10^{-3}$ in non-dashed and 10^{-2} in dashed slopes when $\tau = 50$. Note that $\mathcal{FG}_n$ is excluded from the current study due to its discrete nature (where $0 < H < 1$). We discovered that the current quantitative behavior of purity and von Neumann entropy differs significantly from that observed when g is large. The preservation duration of the phenomenon is substantially longer for minor values of g, as shown. The qualitative degradation behavior is monotonic, as it was in prior situations. In comparison, $\mathcal{OU}_n$ followed by $\mathcal{G}_n$ has had less degrading effects on the purity, coherence, and information survival over a long period. Finally, $\mathcal{PL}_n$ is found to be the most harmful to the dynamics of purity, coherence, and information, with saturation levels being reached earlier, especially for large g values. The single qutrit system's quantitative degradation is minimal and partial, and in contrast, complete coherence losses are observed in different quantum systems under different Markovian and non-Markovian noises; for example, those given in [57,76,77,79,80,86]. Most significantly, we found that the decay rate is greatly regulated by altering the values of g, which directly increases as this parameter is increased. Regardless of the preservation duration and the parameter values, all noises can induce a similar amount of decay. This strongly suggests the relevance of the Gaussian nature of the noises. As shown, following maximum decay, the slopes under all the noises remained at the same elevation levels.

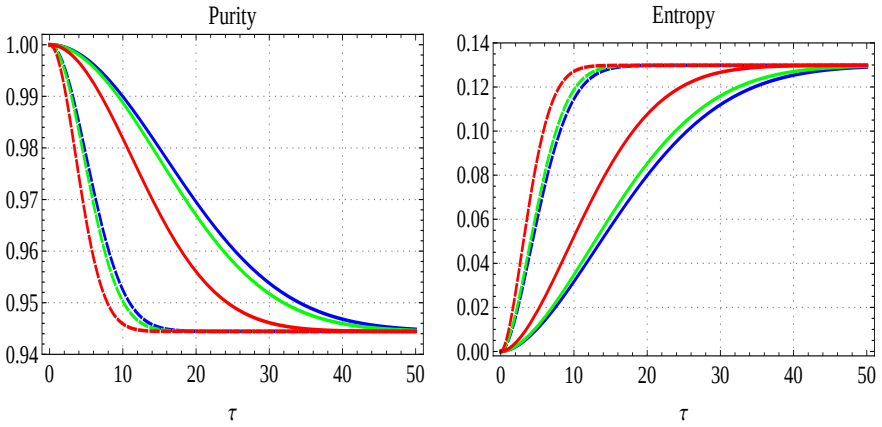

Figure 8. Prolonged preservation of (**a**) purity and (**b**) von Neumann entropy as functions of g versus τ in a single qutrit system under Gaussian (green), Ornstein–Uhlenbeck (blue), and power law noise (red) stemming from the classical field when $g = 10^{-3}$ (non-dashed) and $g = 10^{-2}$ (dashed).

4. Conclusions

When a single qutrit system is exposed to a classical fluctuating field, the symmetrical dynamics of having preserved purity and coherence are studied. The classical fields are driven by a pure Gaussian process, generating several types of Gaussian noise. Furthermore, we also distinguished between noisy and noiseless local fields. Finally, the degrees of pureness, coherence, and information preserved by the single qutrit system are determined using purity and von Neumann entropy.

We show that except for the $\mathcal{FG}_n$, all the noises have displayed similar degrading behaviors in terms of purity, coherence, and information. The decay rates for the current Gaussian noises increased as the noise parameters were raised. On the other hand, as H rises, purity and coherence become robust initially in the case of $\mathcal{FG}_n$. This qualitative behavior of H is unlike that of any other noise parameter previously investigated. In each case, the saturation levels were consistent. This suggests the relevance of the noise phases as having the same Gaussian nature and causing an equal amount of decay. Most significantly, the preservation time remained greater with $\mathcal{OU}_n$ for small g and under $\mathcal{PL}_n$ for small α. In the case of measures, purity and von Neumann entropy were found to be in good agreement. Over an equivalent time duration, the maxima and minima of both metrics are

perfectly concordant. Therefore, purity and von Neumann entropy are accurate indicators of the initial purity, coherence, and information encoded in a quantum system. Finally, under current Gaussian noises, purity and coherence suffer a lesser loss, which is affected significantly by noise parameter values. In contrast to the smaller partial loss of coherence in the current three-level system, non-Gaussian noises appear to destroy coherence over time in quantum systems with a higher number of qubits and qutrits. To reduce this deterioration, the Gaussian noisy parameters should be kept as low as possible. In particular, for $g = 10^{-3}$ and $g = 10^{-2}$, the coherence, information, and in turn, coherence, can be preserved for a long enough interaction time.

Author Contributions: A.u.R. have proposed the main idea and performed the calculations. A.u.R. and S.M.Z. wrote the original draft, while the rest of the authors contributed to the development of the idea, writing and discussions of the manuscript, and analyzing the results. Thorough checking of the paper was done by all authors. All authors have read and agreed to the published version of the manuscript.

Funding: Financial support from the Postdoctoral training funds, grant nos. C615300501.

Data Availability Statement: The data that support the findings of this study are available upon reasonable request from the authors.

Acknowledgments: S. M. Zangi is extremely grateful for the help and support of Bo Zheng.

Conflicts of Interest: The authors declare no conflict of interest.

References

1. Blais, A.; Girvin, S.M.; Oliver, W.D. Quantum information processing and quantum optics with circuit quantum electrodynamics. *Nat. Phys.* **2020**, *16*, 247–256. [CrossRef]
2. Paesani, S.; Borghi, M.; Signorini, S.; Maïnos, A.; Pavesi, L.; Laing, A. Near-ideal spontaneous photon sources in silicon quantum photonics. *Nat. Commun.* **2020**, *11*, 2505 . [CrossRef] [PubMed]
3. Bennett, C.H.; DiVincenzo, D.P. Quantum information and computation. *Nature* **2000**, *404*, 247–255. [CrossRef] [PubMed]
4. Sakajo, T.; Yokoyama, T. Discrete representations of orbit structures of flows for topological data analysis. *Discret. Math. Algorithms Appl.* **2022**, 2250143. [CrossRef]
5. Hirota, O.; Sohma, M.; Fuse, M.; Kato, K. Quantum stream cipher by the Yuen 2000 protocol: Design and experiment by an intensity-modulation scheme. *Phys. Rev. A* **2005**, *72*, 022335. [CrossRef]
6. Gao, X.; Anschuetz, E.R.; Wang, S.T.; Cirac, J.I.; Lukin, M.D. Enhancing generative models via quantum correlations. *Phys. Rev. X* **2022**, *12*, 021037. [CrossRef]
7. Di Vincenzo, D.P.; Loss, D. Quantum computers and quantum coherence. *J. Magn. Magn. Mater.* **1999**, *200*, 202–218. [CrossRef]
8. Napoli, C.; Bromley, T.R.; Cianciaruso, M.; Piani, M.; Johnston, N.; Adesso, G. Robustness of coherence: An operational and observable measure of quantum coherence. *Phys. Rev. Lett.* **2016**, *116*, 150502. [CrossRef]
9. Mansour, M.; Dahbi, Z. Entanglement of bipartite partly non-orthogonal-spin coherent states. *Laser Phys.* **2020**, *30*, 085201. [CrossRef]
10. Mansour, M.; Dahbi, Z.; Essakhi, M.; Salah, A. Quantum correlations through spin coherent states. *Int. J. Theor. Phys.* **2021**, *60*, 2156–2174. [CrossRef]
11. Abd-Rabbou, M.Y.; Metwally, N.; Ahmed, M.M.A.; Obada, A.S. Decoherence and quantum steering of accelerated qubit–qutrit system. *Quantum Inf. Process.* **2022**, *21*, 363. [CrossRef]
12. Hu, M.L.; Hu, X.; Wang, J.; Peng, Y.; Zhang, Y.R.; Fan, H. Quantum coherence and geometric quantum discord. *Phys. Rep.* **2018**, *762*, 1–100. [CrossRef]
13. Wang, X.L.; Yue, Q.L.; Yu, C.H.; Gao, F.; Qin, S.J. Relating quantum coherence and correlations with entropy-based measures. *Sci. Rep.* **2017**, *7*, 12122. [CrossRef] [PubMed]
14. Bloch, I. Quantum coherence and entanglement with ultracold atoms in optical lattices. *Nature* **2008**, *453*, 1016–1022. [CrossRef] [PubMed]
15. Zurek, W.H. Preferred states, predictability, classicality and the environment-induced decoherence. *Prog. Theor. Phys.* **1993**, *89*, 281–312. [CrossRef]
16. Rahman, A.U.; Javed, M.; Ji, Z.; Ullah, A. Probing multipartite entanglement, coherence and quantum information preservation under classical Ornstein-Uhlenbeck noise. *J. Phys. A Math. Theor.* **2021**, *55*, 025305. [CrossRef]
17. Rahman, A.U.; Noman, M.; Javed, M.; Ullah, A.; Luo, M.X. Effects of classical fluctuating environments on decoherence and bipartite quantum correlations dynamics. *Laser Phys.* **2021**, *31*, 115202. [CrossRef]
18. Rahman, A.U.; Ji, Z.X.; Zhang, H.G. Demonstration of entanglement and coherence in GHZ-like state when exposed to classical environments with power-law noise. *Eur. Phys. J. Plus* **2022**, *137*, 440. [CrossRef]

19. Rahman, A.U.; Zidan, N. Quantum memory assisted entropic uncertainty and entanglement dynamics in classical dephasing channels. *arXiv* **2021**, arXiv:2111.11312.
20. Rahman, A.U.; Javed, M.; Kenfack, L.T.; Safi, S.K. Multipartite quantum correlations and coherence dynamics subjected to classical environments and fractional Gaussian noise. *arXiv* **2021**, arXiv:2111.02220.
21. Abd-Rabbou, M.Y.; Khan, S.; Shamirzaie, M. Quantum fisher information and quantum coherence of an entangled bipartite state interacting with a common classical environment in accelerating frames. *Quantum Inf. Process.* **2022**, *21*, 218. [CrossRef]
22. Omri, M.; Abd-Rabbou, M.Y.; Khalil, E.M.; Abdel-Khalek, S. Thermal information and teleportation in two-qutrit Heisenberg XX chain model. *Alex. Eng. J.* **2022**, *61*, 8335–8342. [CrossRef]
23. Abd-Rabbou, M.Y.; Ali, S.I.; Ahmed, M.M.A. Enhancing the information of nonlinear SU (1, 1) quantum systems interacting with a two-level atom. *Opt. Quantum Electron.* **2022**, *548*, 548. [CrossRef]
24. Haddadi, S.; Ghominejad, M.; Akhound, A.; Pourkarimi, M.R. Entropic uncertainty relation and quantum coherence under Ising model with Dzyaloshinskii–Moriya interaction. *Laser Phys. Lett.* **2021**, *18*, 085204. [CrossRef]
25. Rahman, A.U.; Haddadi, S.; Pourkarimi, M.R. Tripartite Quantum Correlations under Power-Law and Random Telegraph Noises: Collective Effects of Markovian and Non-Markovian Classical Fields. *Ann. Der Phys.* **2022**, *534*, 2100584. [CrossRef]
26. Mallick, K.; Marcq, P. On the stochastic pendulum with Ornstein–Uhlenbeck noise. *J. Phys. Math. Gen.* **2004**, *37*, 4769. [CrossRef]
27. Koutsoyiannis, D. The Hurst phenomenon and fractional Gaussian noise made easy. *Hydrol. Sci. J.* **2002**, *47*, 573–595. [CrossRef]
28. Benedetti, C.; Paris, M.G. Characterization of classical Gaussian processes using quantum probes. *Phys. Lett. A* **2014**, *378*, 2495–2500. [CrossRef]
29. Toth, G.; Apellaniz, I. Quantum metrology from a quantum information science perspective. *J. Phys. A Math. Theor.* **2014**, *47*, 424006. [CrossRef]
30. Liu, J.; Yuan, H.; Lu, X.M.; Wang, X. Quantum Fisher information matrix and multiparameter estimation. *J. Phys. A Math. Theor.* **2019**, *53*, 023001. [CrossRef]
31. Javed, M.; Khan, S.; Ullah, S.A. Characterization of classical static noise via qubit as probe. *Quantum Inf. Process.* **2018**, *17*, 53. [CrossRef]
32. Kenfack, L.T.; Tchoffo, M.; Fai, L.C. Estimation of the disorder degree of the classical static noise using three entangled qubits as quantum probes. *Phys. Lett. A* **2019**, *383*, 1123–1131. [CrossRef]
33. Lu, X.M.; Wang, X.; Sun, C.P. Quantum Fisher information flow and non-Markovian processes of open systems. *Phys. Rev. A* **2010**, *82*, 042103. [CrossRef]
34. Li, N.; Luo, S. Entanglement detection via quantum Fisher information. *Phys. Rev. A* **2013**, *88*, 014301. [CrossRef]
35. Streltsov, A.; Singh, U.; Dhar, H.S.; Bera, M.N.; Adesso, G. Measuring quantum coherence with entanglement. *Phys. Rev. Lett.* **2015**, *115*, 020403. [CrossRef]
36. Hu, M.; Zhou, W. Enhancing two-qubit quantum coherence in a correlated dephasing channel. *Laser Phys. Lett.* **2019**, *16*, 045201. [CrossRef]
37. Nirwan, R.S.; Bertschinger, N. Applications of Gaussian process latent variable models in finance. In Proceedings of the SAI Intelligent Systems Conference, London, UK, 5–6 September 2019; Springer: Cham, Switzerland, 2019; pp. 1209–1221.
38. Lazaro-Gredilla, M.; Titsias, M.K. Variational heteroscedastic Gaussian process regression. In Proceedings of the ICML, Bellevue, WA, USA, 28 June–2 July 2011.
39. Schwab, D. Efficacy of Gaussian Process Regression for Angles-Only Initial Orbit Determination. Master's Thesis, Penn State University, State College, PA, USA, 2020.
40. Sharifzadeh, M.; Sikinioti-Lock, A.; Shah, N. Machine-learning methods for integrated renewable power generation: A comparative study of artificial neural networks, support vector regression, and Gaussian Process Regression. *Renew. Sustain. Energy Rev.* **2019**, *108*, 513–538. [CrossRef]
41. Ibrahim, S.K.; Ahmed, A.; Zeidan, M.A.E.; Ziedan, I.E. Machine learning methods for spacecraft telemetry mining. *IEEE Trans. Aerosp. Electron. Syst.* **2018**, *55*, 1816–1827. [CrossRef]
42. Rodrigues, F.; Pereira, F.; Ribeiro, B. Gaussian process classification and active learning with multiple annotators. In Proceedings of the International Conference on Machine Learning, PMLR, Bejing, China, 22–24 June 2014; pp. 433–441.
43. Taqqu, M.S.; Teverovsky, V.; Willinger, W. Estimators for long-range dependence: An empirical study. *Fractals* **1995**, *3*, 785–798. [CrossRef]
44. Prasad, S.K.; Aghajarian, D.; McDermott, M.; Shah, D.; Mokbel, M.; Puri, S.; Wang, S. Parallel processing over spatial-temporal datasets from geo, bio, climate and social science communities: A research roadmap. In Proceedings of the 2017 IEEE International Congress on Big Data (BigData Congress), Honolulu, HI, USA, 25–30 June 2017; pp. 232–250.
45. Pelletier, J.D.; Turcotte, D.L. Long-range persistence in climatological and hydrological time series: Analysis, modelling and application to drought hazard assessment. *J. Hydrol.* **1997**, *203*, 198–208. [CrossRef]
46. Maxim, V.; Şendur, L.; Fadili, J.; Suckling, J.; Gould, R.; Howard, R.; Bullmore, E. Fractional Gaussian noise, functional MRI and Alzheimer's disease. *Neuroimage* **2005**, *25*, 141–158. [CrossRef] [PubMed]
47. Paxson, V. Fast, approximate synthesis of fractional Gaussian noise for generating self-similar network traffic. *ACM SIGCOMM Comput. Commun. Rev.* **1997**, *27*, 5–18. [CrossRef]
48. De Moura, C.E.; Pizzinga, A.; Zubelli, J. A pairs trading strategy based on linear state space models and the Kalman filter. *Quant. Financ.* **2016**, *16*, 1559–1573. [CrossRef]

49. Blekos, K.; Stefanatos, D.; Paspalakis, E. Performance of superadiabatic stimulated Raman adiabatic passage in the presence of dissipation and Ornstein-Uhlenbeck dephasing. *Phys. Rev. A* **2020**, *102*, 023715. [CrossRef]
50. Koch, C.P.; Boscain, U.; Calarco, T.; Dirr, G.; Filipp, S.; Glaser, S.J.; Wilhelm, F.K. Quantum optimal control in quantum technologies. Strategic report on current status, visions and goals for research in Europe. *EPJ Quantum Tech.* **2022**, *9*, 19.
51. Stefanatos, D.; Paspalakis, E. A shortcut tour of quantum control methods for modern quantum technologies. *Europhys. Lett.* **2021**, *132*, 60001. [CrossRef]
52. Burgess, A.E.; Judy, P.F. Signal detection in power-law noise: Effect of spectrum exponents. *J. Opt. Soc. Am. A* **2007**, *24*, B52–B60. [CrossRef] [PubMed]
53. Burgess, A.E.; Jacobson, F.L.; Judy, P.F. Human observer detection experiments with mammograms and power-law noise. *Med. Phys.* **2001**, *28*, 419–437. [CrossRef]
54. Lam, C.H.; Sander, L.M. Surface growth with power-law noise. *Phys. Rev. Lett.* **1992**, *69*, 3338. [CrossRef]
55. Molina-Garcia, D.; Sandev, T.; Safdari, H.; Pagnini, G.; Chechkin, A.; Metzler, R. Crossover from anomalous to normal diffusion: Truncated power-law noise correlations and applications to dynamics in lipid bilayers. *New J. Phys.* **2018**, *20*, 103027. [CrossRef]
56. Abd-Rabbou, M.Y.; Metwally, N.; Ahmed, M.M.A.; Obada, A.S. Wigner function of noisy accelerated two-qubit system. *Quantum Inf. Process.* **2019**, *18*, 367. [CrossRef]
57. Rossi, M.A.; Benedetti, C.; Paris, M.G. Engineering decoherence for two-qubit systems interacting with a classical environment. *Int. J. Quantum Inf.* **2014**, *12*, 1560003. [CrossRef]
58. Masoomy, H.; Askari, B.; Najafi, M.N.; Movahed, S.M.S. Persistent homology of fractional Gaussian noise. *Phys. Rev. E* **2021**, *104*, 034116. [CrossRef] [PubMed]
59. Ledesma, S.; Liu, D. Synthesis of fractional Gaussian noise using linear approximation for generating self-similar network traffic. *ACM SIGCOMM Comput. Commun. Rev.* **2000**, *30*, 4–17. [CrossRef]
60. Luft, M.; Cioc, R.; Pietruszczak, D. Fractional calculus in modelling of measuring transducers. *Elektron. Elektrotech.* **2011**, *110*, 97–100. [CrossRef]
61. Guo, X.; Liu, F.; Tian, X. Gaussian noise level estimation for color image denoising. *JOSA A* **2021**, *38*, 1150–1159. [CrossRef]
62. Merhav, N.; Guo, D.; Shamai, S. Statistical physics of signal estimation in Gaussian noise: Theory and examples of phase transitions. *IEEE Trans. Inf. Theory* **2010**, *56*, 1400–1416. [CrossRef]
63. Amar, J.G.; Family, F. Scaling of surface fluctuations and dynamics of surface growth models with power-law noise. *J. Phys. A Math. Gen.* **1991**, *24*, L79. [CrossRef]
64. Kasdin, N.J. Discrete simulation of colored noise and stochastic processes and 1/f/sup/spl alpha//power law noise generation. *Proc. IEEE* **1995**, *83*, 802–827. [CrossRef]
65. Zhao, M.J.; Ma, T.; Quan, Q.; Fan, H.; Pereira, R. l_1-norm coherence of assistance. *Phys. Rev. A* **2019**, *100*, 012315. [CrossRef]
66. Mazzola, L.; Piilo, J.; Maniscalco, S. Frozen discord in non-Markovian dephasing channels. *Int. J. Quantum Inf.* **2011**, *9*, 981–991. [CrossRef]
67. Benedetti, C.; Paris, M.G.; Buscemi, F.; Bordone, P. Time-evolution of entanglement and quantum discord of bipartite systems subject to $1/f^{\alpha}$ noise. In Proceedings of the 2013 22nd International Conference on Noise and Fluctuations (ICNF), Montpellier, France, 24–28 June 2013; pp. 1–4.
68. Kenfack, L.T.; Tchoffo, M.; Javed, M.; Fai, L.C. Dynamics and protection of quantum correlations in a qubit–qutrit system subjected locally to a classical random field and colored noise. *Quantum Inf. Process.* **2020**, *19*, 1–26. [CrossRef]
69. Essakhi, M.; Khedif, Y.; Mansour, M.; Daoud, M. Intrinsic decoherence effects on quantum correlations dynamics. *Opt. Quantum Electron.* **2022**, *54*, 103. [CrossRef]
70. Benedetti, M.; Garcia-Pintos, D.; Perdomo, O.; Leyton-Ortega, V.; Nam, Y.; Perdomo-Ortiz, A. A generative modeling approach for benchmarking and training shallow quantum circuits. *NPJ Quantum Inf.* **2019**, *5*, 45. [CrossRef]
71. Sweke, R.; Wilde, F.; Meyer, J.J.; Schuld, M.; Fährmann, P.K.; Meynard-Piganeau, B.; Eisert, J. Stochastic gradient descent for hybrid quantum-classical optimization. *Quantum* **2020**, *4*, 314. [CrossRef]
72. Ji, Z.; Zhang, H.; Wang, H.; Wu, F.; Jia, J.; Wu, W. Quantum protocols for secure multi-party summation. *Quantum Inf. Process.* **2019**, *18*, 168. [CrossRef]
73. Khedif, Y.; Haddadi, S.; Pourkarimi, M.R.; Daoud, M. Thermal correlations and entropic uncertainty in a two-spin system under DM and KSEA interactions. *Mod. Phys. Lett. A* **2021**, *36*, 2150209. [CrossRef]
74. Haddadi, S.; Pourkarimi, M.R.; Haseli, S. Relationship between quantum coherence and uncertainty bound in an arbitrary two-qubit X-state. *Opt. Quantum Electron.* **2021**, *53*, 529. [CrossRef]
75. Khedif, Y.; Daoud, M.; Sayouty, E.H. Thermal quantum correlations in a two-qubit Heisenberg XXZ spin-chain under an inhomogeneous magnetic field. *Phys. Scr.* **2019**, *94*, 125106. [CrossRef]
76. Yu, T.; Eberly, J.H. Sudden death of entanglement: Classical noise effects. *Opt. Commun.* **2006**, *264*, 393–397. [CrossRef]
77. Kenfack, L.T.; Tchoffo, M.; Fai, L.C.; Fouokeng, G.C. Decoherence and tripartite entanglement dynamics in the presence of Gaussian and non-Gaussian classical noise. *Phys. B Condens. Matter* **2017**, *511*, 123–133. [CrossRef]
78. Rahman, A.U.; Noman, M.; Javed, M.; Luo, M.X.; Ullah, A. Quantum correlations of tripartite entangled states under Gaussian noise. *Quantum Inf. Process.* **2021**, *20*, 290. [CrossRef]
79. Rahman, A.U.; Javed, M.; Ullah, A.; Ji, Z. Probing tripartite entanglement and coherence dynamics in pure and mixed independent classical environments. *Quantum Inf. Process.* **2021**, *20*, 321. [CrossRef]

80. Rahman, A.U.; Noman, M.; Javed, M.; Ullah, A. Dynamics of bipartite quantum correlations and coherence in classical environments described by pure and mixed Gaussian noises. *Eur. Phys. J. Plus* **2021**, *136*, 846. [CrossRef]
81. Rossi, M.A.; Paris, M.G. Non-Markovian dynamics of single-and two-qubit systems interacting with Gaussian and non-Gaussian fluctuating transverse environments. *J. Chem. Phys.* **2016**, *144*, 024113. [CrossRef] [PubMed]
82. Buscemi, F.; Bordone, P. Time evolution of tripartite quantum discord and entanglement under local and nonlocal random telegraph noise. *Phys. Rev. A* **2013**, *87*, 042310. [CrossRef]
83. Weinstein, Y.S. Tri-partite Entanglement Witnesses and Sudden Death. *arXiv* **2008**, arXiv:0812.4612.
84. Hao, Y.; Lian-Fu, W. Correlation dynamics of two-parameter qubit—Qutrit states under decoherence. *Chin. Phys. B* **2013**, *22*, 050303.
85. Shamirzaie, M.; Khan, S. The Dynamics of Three Different Entropic Measures of Quantum Correlations in Mixed Bipartite State Coupled with Classical Environments. *Fluct. Noise Lett.* **2018**, *17*, 1850023. [CrossRef]
86. Rahman, A.U.; Khedif, Y.; Javed, M.; Ali, H.; Daoud, M. Characterizing Two-Qubit Non-Classical Correlations and Non-Locality in Mixed Local Dephasing Noisy Channels. *Ann. Der Phys.* **2022**, *534*, 2200197. [CrossRef]